35. A REVIEW OF HYPERSONIC CRUISE VEHICLES

By David E. Fetterman, Charles H. McLellan, L. Robert Jackson,
Beverly Z. Henry, Jr., and John R. Henry
Langley Research Center

SUMMARY

In an attempt to provide a focus for future aerodynamic programs in the development of hydrogen-fueled hypersonic cruise vehicles, the present status of the structural, propulsive, and aerodynamic research is examined to extract the presently known factors that significantly affect vehicle definition. Existing wing and body structural concepts and cryogenic-tankage thermal-protection systems are illustrated, possible inlet-engine arrangements are discussed, and the status of important local aerodynamic heating areas is briefly reviewed. In addition, uncertain areas which require further fundamental research and obstacles which hinder development are also pointed out.

In general, existing structural and propulsive technologies for Mach 6 to 8 vehicles favor a discrete low-wing—body arrangement with a two-dimensional inlet mounted in the wing pressure field. Aerodynamic considerations, however, indicate equal performance possibilities for either discrete wing-body or blended wing-body arrangements. The paper concludes with a discussion of several possible design concepts which conform to current guidelines and which are planned for future research.

INTRODUCTION

Prior to 1957 the only means of propulsion seriously considered for hypersonic flight was the large rocket engine. Thus, the "boost-glide" type of vehicle received almost exclusive attention during the first decade of hypersonic technology development. (See refs. 1 to 5.) With the beginning of space activities in 1957, the magnitude of the launch-vehicle problem began to be appreciated and studies of reusable launch systems were undertaken with the hope of obtaining cheaper and more effective alternates to ballistic rocket boosters. During this time the air-breathing engine came under exhaustive scrutiny as the most obvious alternative to rocket boosters, and a dramatic family of air-breathing vehicles designated "aerospaceplanes" became the subject of intensive study. (See refs. 6 to 15.) Although these conceptual vehicles proved to be premature, there emerged from these studies by 1962 the first clear indications that hypersonic air-breathing propulsion using hydrogen fuel was feasible and attractive up to Mach numbers of about 8 in the form of the subsonic-combustion turboramjet, and up to Mach 12 or higher with the subsonic-supersonic-combustion turboramjet. With this important capability, the possibility of cruise vehicles capable of sustained hypersonic flight also became apparent. (See refs. 16 and 17.)

The hypersonic cruise vehicle is vastly more complex than other hypersonic vehicles such as the boost-glider or the manned reentry vehicle. Its large liquid hydrogen fuel requirement coupled with its air-breathing engines which must provide take-off, acceleration, hypersonic cruise, and subsonic loiter capabilities introduce many difficult new problems. In examining comparative vehicle studies of different design teams, it is apparent that the present state of the art is characterized by large uncertainties. An analysis of these studies reveals that these uncertainties are rooted partly in aerodynamic predictions for complete configurations, partly in the attainable weight fractions of cryogenic and high-temperature structures, and partly in the installed performance of hypersonic propulsion systems. Within the spread of these uncertainties, results for particular missions can be found which range all the way from attractive to unattractive vehicle systems. The technology for air-breathing hypersonic cruise and boost vehicles is thus in the same early stage as supersonic transport technology was some dozen or so years ago when serious studies of complete realistic aerodynamic configurations, structures, and engines were just beginning. In order to reduce the present uncertainties in the state of the art, extensive programs are now getting underway in both USAF and NASA.

At the present early stage in the development of these vehicles, any meaningful discussion of configuration concept becomes involved with questions of structures, materials, and propulsion, since each of these technological areas can have a significant influence on the shaping of the vehicle. To obtain realistic results that significantly advance vehicle development, the aerodynamic programs, then, must be properly focused on configurations which reflect these influences. To aid in this focusing process, this paper briefly examines the structural, propulsive, and aerodynamic disciplines in that order and sets forth the presently known factors affecting vehicle shape. Singled out along the way will be uncertain areas which require more work and the obstacles which hinder development and must be overcome. The paper concludes with several possible design concepts which should be investigated in future programs. For reasons which will become apparent, vehicles in the Mach 6 to 8 class and those for higher Mach numbers of about 12 are significantly different. During the discussion Mach 6 and Mach 12 are used to refer to the two speed classes.

Although this paper treats only the cruise vehicle, it should be noted that many points of commonalty exist between cruise and launch vehicles. (See ref. 14.) Much of the information contained herein for cruise vehicles, therefore, applies to the others as well.

CHARACTERISTICS OF HYPERSONIC CRUISE VEHICLES

The environment in which a hypersonic cruise vehicle (HCV) operates is shown by the flight profile. The flight profile is subject to the various constraints shown in figure 1. Preliminary studies (discussed in paper no. 29 by McLean, Carlson, and Hunton) of the sonic-boom constraint indicate that because of the larger vehicles involved, the problem is more severe for the HCV at lower speeds than for the supersonic transport (SST), but because of the higher altitudes is less severe during cruise. The vehicle then follows a constant dynamic

pressure path. The highest possible dynamic pressures are desirable for improved propulsion performance; however, from the structural standpoint, low dynamic pressures are desirable to alleviate panel flutter and the heating problems denoted by the constant peak skin temperature lines. For subsonic-combustion ramjet propulsion systems, the inlet duct pressures must be limited to avoid excessive propulsion-system weight and flight paths are constrained to constant duct pressure lines. In supersonic-combustion ramjet engines, of course, the internal duct pressures are much lower and this duct pressure limitation is eliminated.

A typical trajectory for a Mach 6 cruise vehicle follows a peak dynamic pressure path of 1500 psf with cruise occurring between 800 and 500 psf. Peak skin temperatures 3 feet aft of the leading edge are about 1500° F. The descent phase of the flight is made at altitudes high enough to avoid the climb phase constraints.

Because of the conflicting trajectory requirements of structures, propulsion, and aerodynamics, a large interplay among these areas exists in the design of hypersonic cruise vehicles. As a first step in defining efficient vehicle systems, it is essential, therefore, to perform analytic trade-off studies in which the key parameters in structures, propulsion, and aerodynamics are systematically varied. These studies have been conducted within NASA (ref. 16) and under contract, and these results have provided a preliminary indication of the more important vehicle characteristics. These results, compared with those for the SST, are shown in table I. Symbols appearing in the table and the figures are defined in the appendix.

These trade-off studies considered a cruise Mach number of 6 and assumed a range of 5500 n. mi. and a gross weight equal to that of the SST. Shorter ranges, such as that of the SST, are less attractive for hypersonic transports because most of the trip would be taken up by acceleration and deceleration and little trip-time advantage is found. Studies of JP-fueled hypersonic cruise vehicles indicate that only about half the desired range is available (ref. 17); thus, the use of hydrogen fuel is the dominant requirement of these vehicles. The desired range can then be achieved with about the same payload weight as for the SST but with a lower fuel weight. The low density of hydrogen, however, requires a fuel volume about an order of magnitude larger than that required for the SST. The structural problems involved in housing the liquid hydrogen and designing for the higher temperature environment result in structural weight fractions some 30 percent greater than for the SST. This more severe structural problem causes HCV performance to be optimized with aerodynamic configurations which are much less slender than the SST. A comparison of HCV and SST vehicles is shown in figure 2. The fuselage fineness ratios are about half those for the SST and the hypersonic L/D is about 5, a value which is below that obtainable at hypersonic speeds for more slender designs. The wing loadings tend to be in the same range as for the SST because take-off and sonic-boom considerations size the wing in both vehicles.

STRUCTURES

A configuration which embodies most of the design features preferred in present structural technology is shown in figure 3. Probably the most significant structural design influence involves the manner in which the liquid hydrogen is contained in the vehicle. At hypersonic conditions an extreme temperature difference of about 2000° F exists between the inner wall of the fuel tank and the outer surface of the vehicle. (See ref. 18.) The cryogenic structural problem is presently one of the main concerns. One solution under extensive study is the nonintegral tankage approach shown in figure 3 wherein the fuel tanks are separate from the load-bearing structure. With this concept, cylindrical and conical tanks are preferred; and structural design favors discrete wing-body arrangements with the wing located over or beneath the body to avoid interference between the wing carry-through structure and the tankage.

To allow lower wing weights, a fuselage-mounted vertical fin may be preferred to wing-tip fins; and to allow thermal expansion on the hot leading edges, a segmented, overlapping leading edge on the tail and wing is required rather than the smooth unit used on the SST. Leading-edge temperatures for Mach 6 vehicles can be held to less than 2200° F and coated thoriated nickel (ref. 18) is a possible leading-edge material which requires only infrequent refurbishment. However, for Mach 12 vehicles coated refractories such as columbium will have to be used (ref. 19) and frequent leading-edge refurbishment will be required. At Mach 6 the wing maximum surface temperatures are generally less than 1600° F, and the major part of the wing can be constructed of superalloy materials using stress-skin construction similar to that used on the SST.

The surface roughness conditions prescribed in flight are of importance both from configuration performance and local aerodynamic heating considerations. At one time it was believed that the surfaces of hypersonic vehicles would be covered with large buckles and discontinuities brought about by thermal stress and expansion. Structural concepts have been devised to minimize these distortions, and a concept for Mach 6 vehicles is shown in figure 4.

The leading edge is shown detached, and it includes the entire area behind the leading edge itself over which temperatures are in excess of 1600° F. The load-bearing skin is waffle stiffened and stabilized by corrugated webs and spars to prevent buckling. Thermal stress is reduced by exposing the spar and rib caps. With this structural concept, it is expected that the surface will be almost as smooth as that on the SST. The only significant discontinuity will be steps, on the order of 0.020 inch, located at the edges of the leading-edge segments and at the juncture of the leading edge and the wing. If the steps are facing away from the local flow, however, they should not present a serious problem.

If designs for the Mach 12 range are considered, higher temperatures occur over large surface areas of the wing and a structural concept of the type shown in figure 5 is required. A shingled nonload-bearing exterior heat shield and insulation system must now be added to a basic wing and body structure to

maintain its operation at temperatures not in excess of 1600° F. Corrugated heat-protective shingles form the outer surface and large surface irregularities will occur. It is a mistake to assume that by running these corrugations "streamwise" their effect can be ignored. Actually the local flow directions on bodies and delta wings vary significantly with angle of attack and, therefore, cross flows over the corrugations will inevitably be encountered. The aerodynamic and heating consequences of this are not yet known but are almost certainly significant. Further research in high-temperature structures aimed at smoother shingles without excessive weight is needed.

Since the trade-off study results (table I and fig. 2) are sensitive to structural weight, the hydrogen-fuel tankage structure and insulation weight can have important implications on the proportions of the optimum configuration. A reduction in this weight would shift the fuselage fineness ratio to higher values with resulting increases in configuration $(L/D)_{max}$. Possible structural concepts for nonintegral tankage are shown in figure 6.

The storage of high volumes of liquid hydrogen fuel within structures subject to high external heating presents major new problems. The cold tankage must not only be heavily insulated to prevent fuel losses, but purging must also be provided to avoid air and water condensation (ref. 20) between tank and structure and to remove any hydrogen leakage. In the upper left of figure 6, this purging is accomplished by helium. The basic difficulty here is the large weight of the thermal protection system and helium purge system required. Additional weight due to the need for a coolant system, particularly at Mach numbers greater than 8, to reduce tank temperatures in "dry" areas after the fuel has been partially used may also have to be included.

A scheme under test at Langley which may provide significant reduction in thermal protection and purge system weight is shown at the lower right in figure 6. (See ref. 21.) A CO_2 frost is cryo-deposited within the inner thickness of fibrous insulation during ground hold prior to flight. During flight the frost sublimes and provides the purge gas. The sublimation process eliminates the need for an additional coolant system for the dry tank walls. A large model of this concept shown in figure 7 has been built and is scheduled for radiation-heating tests. The model is scheduled for testing in the Langley 8-foot high-temperature structures tunnel at Mach 7.

Another approach based on the concept of "integral" tankage is also under study at Langley Research Center. In principal, cooling of the load-bearing structure by the fuel might result in weight saving. A large model incorporating the integral or evacuated "multiwall" structural concept (ref. 21) is shown in figure 8. Great difficulties have been encountered in developing this model, particularly in obtaining the required vacuum in the thin-gage elements. Helium purge gas is shown in the structural portion of the sandwich wall to detect fuel leakage. The purge-gas requirements are uncertain but may be sizable. Further research on evacuated heat shields is needed to develop improved techniques and to determine the reliability with which thin-gage materials can be sealed.

The integral tankage structure encounters an additional problem in the joining of the cold tank structure and the hot wing structure. It is too early to say whether a significant weight penalty is involved here or whether merged wing-body arrangements can be found which are attractive for the use of integral tankage.

The propulsion unit, shown by the simple schematic in figure 3, is actually a very complex, specialized structural problem. The unit contains the inlet duct and a combination engine consisting of a turbojet for acceleration to about Mach 3 and a ramjet for acceleration to Mach 6. At higher speeds a supersonic-combustion ramjet (scramjet) engine must also be provided. No materials are now available to withstand the extreme temperatures occurring on the turbine blades under stoichiometric operation at Mach 3 and those generated in the inlet duct and ramjet combustion chamber at higher Mach numbers. Active cooling of these surfaces by the liquid hydrogen fuel is, therefore, required. The cooling problem presents one of the major challenges in the structural design of these units.

PROPULSION

Typical propulsion-system installations for Mach 6 cruise vehicles are shown in figure 9. One possible type of turbo-accelerator ramjet is shown in which a switching valve redirects the airflow to either the turbojet or the subsonic-combustion ramjet. These combination engines allow a common inlet to be used for both the turbojet and ramjet.

An axisymmetric pod arrangement as used on lower speed cruise vehicles is shown at the top of the figure. This arrangement has advantages of low weight and absence of contaminating boundary layers from adjacent surfaces. Regenerative fuel cooling of the entire internal ducting and external cowl lip will be required. The spike may be either radiation cooled or fuel cooled. Large spike translations are essential to achieve adequate performance throughout the speed range. The two-dimensional installation more readily incorporates the requisite variable geometry through the adjustable wall. However, it may require a more elaborate boundary-layer bleed system including a diverter to prevent the thick wing-body boundary layer from entering the duct.

A question of major importance in configuration definition is the inlet size requirement of these installations. Factors that affect inlet size are the vehicle aerodynamic characteristics, efficiency of the engine-inlet combination, location of the inlet on the vehicle, flight path, and minimum acceleration criteria along the flight path. Representative calculations have been made for Mach 6 and Mach 8 cruise vehicles by using the method of reference 22 to define inlet size requirements and the attendant longitudinal-acceleration characteristics. The calculations assumed that the vehicle would cruise at $(L/D)_{max}$. The propulsion system assumed a subsonic combustion turboramjet engine in conjunction with two inlet types located in the wing pressure field: the first was assumed to operate at full capture at cruise with flow spillage

through a fixed 6° wedge shock at lower speeds, whereas the second type was assumed to operate at full capture at all speeds.

The flight-path constraints (see fig. 10) included a transonic acceleration altitude of 40 000 feet, a dynamic pressure limit of 1500 psf, and an inlet duct pressure limit of 200 psi. For the conditions assumed, the Mach 6 cruise altitude lies above the acceleration path and a constant Mach number climb to this altitude is performed. For the Mach 8 case, the cruise altitude lies below the acceleration path and the final acceleration is performed at cruise altitude at reduced inlet pressure recovery to conform to the duct pressure limit.

The flight aerodynamic characteristics are depicted in figure 11. For most of the acceleration phase, the vehicle system operates well below maximum lift-drag ratio, reaching this condition in a brief portion of the subsonic climb and at the cruise condition. The final portion of the Mach 8 acceleration path is flown at very nearly $(L/D)_{max}$ as a result of the characteristics imposed by the duct-pressure-limit assumption.

The acceleration characteristics are shown in figure 12. The higher accelerations are for the inlet operating at full capture at all conditions, with the higher thrust levels a consequence of the higher airflow characteristics of these inlets. As noted previously, the actual inlet will probably fall between these extremes.

The accelerations were provided by sizing the ramjet and inlet area for the condition at the start of cruise. This inlet area was then used over the flight path and the turbojet portion of the engine was sized to provide minimum acceleration of 2 ft/sec^2 at transonic speeds. With these inlet-engine sizing criteria, an average acceleration level of about 0.2g over the Mach number range is provided, a level which is several times larger than SST values but in the range needed to achieve adequately short acceleration periods for Mach 6 cruise. The inlet areas required were less than 2 percent of the wing area.

The location of these inlets also has an important influence on vehicle shaping. In figure 13 the inlet area required to obtain various accelerations is shown for two cases - when the inlet can be located in the wing compression field, as for the previous calculations, and when the inlet ingests free-stream air. At angle of attack the air beneath the wing is precompressed and this advantage results in a small enough inlet at near-zero acceleration to be located in this pressure field as shown. There is a usable limit, however, to the inlet size that can be contained in this preferred location; and this limit on a delta wing for a two-dimensional inlet of realistic length is shown by the shaded region. For higher acceleration (or higher Mach number) vehicles where the inlet may be too large to be located in the wing pressure field, the upper curves may dictate required inlet areas, and because the inlet now must furnish all the compression it becomes large enough to house both fuel and payload. The aircraft must now be designed around the inlet and a "flying inlet" configuration results. These "flying engine" types will utilize scramjet propulsion beyond Mach 8 where, for a number of reasons, the subsonic-combustion ramjet performance deteriorates rapidly with increased speed.

Both USAF and NASA have sizable programs for hypersonic ramjet development. The NASA work centers on the development of an 18-inch-diameter engine capable of both subsonic and supersonic burning. It will eventually be flight tested to Mach 8 on an uprated X-15 airplane. The first phase of this project, which is now finished, included engine concept development and evaluation in depth. One of the results of these studies is a detailed evaluation of the regenerative fuel-cooling requirements; these are shown in figure 14.

The fuel flow for cooling is shown as a fraction of the fuel required for propulsion with stoichiometric burning. For values of this ratio up to 1, the fuel carried for propulsion is sufficient for cooling purposes. For ratios above 1, additional fuel must be carried to meet cooling needs.

The study results (shown in fig. 14) have been extrapolated, using Reynolds number corrections, for an engine of 7-foot diameter. At Mach 6 adequate fuel is available for cooling; however, cooling needs increase rapidly with Mach number and near 7 it is questionable whether sufficient fuel for cooling is available. Beyond Mach 7 the cooling requirements become severe, and there is strong evidence from these studies that these cooling requirements may constitute a more serious obstacle to higher flight speeds than the problems of aerodynamics, supersonic combustion, or even structures. Opportunities for improving the situation, however, exist if the allowable duct wall temperatures can be increased and/or shorter engines with lower wetted surfaces developed.

A major concern of the aerodynamicist is the increase in drag and the interference effects that result when propulsion systems are added to the airframe. Little significant hypersonic experimental work in this area has been reported in the literature. An investigation by Frank S. Kirkham and William J. Small has recently been performed in the Langley 11-inch hypersonic tunnel at Mach 6.8 on the models equipped with two-dimensional and pod inlets shown in figure 15. Flow-through inlets were used, and the ramp and spikes were not included. The inlet areas for both types were 1.8 percent of the wing area, which is in the right range for Mach 6 cruise vehicles, and both inlets captured the precompressed air beneath the wing. The results show the increase in total drag due to inlet addition at an angle of attack of 6° which is close to that for $(L/D)_{max}$.

The theoretical results, which include pressure and both internal and external skin-friction drag, are in good agreement with experimental results for the two-dimensional inlet. With pod inlets a much larger drag increase occurs and only about half the increment is predicted. The difference is due to the greater interference effects between the pod inlets and the airframe. The calculated increase in internal inlet drag, which is not chargeable to total drag, amounted to about 3 percent for the two-dimensional inlet and 7 percent for the pod inlets.

The extent of these interference effects is indicated in figure 16 which contains oil-flow patterns in the vicinity of the two types of inlets. The flow about the two-dimensional inlet appears very uniform whereas large disturbances from interacting flow fields occur for the pod installations. In addition to excessive interference drag, local heating increases may be more severe

for the pod installations. If the ramp and spikes had been included, they would not have caused additional interference drag under design conditions since the compression shock would be captured by the inlet lip. The off-design conditions, however, are a matter for further study.

These drag and oil-flow results indicate the superiority of two-dimensional inlet installations; however, it should be remembered that these are early results obtained under laminar-boundary-layer conditions. Additional work is required to determine whether similar effects prevail under turbulent flow conditions and whether some benefit can be gained from the interaction effects on pod installations.

AERODYNAMICS

Overall Configuration Considerations

To determine the influence of aerodynamics on vehicle shaping, the findings of basic configuration studies must be referred to since no definitive results are as yet available from complete configuration studies. In examining these basic study results, the main inquiry is concerned with whether any particular family of wing-body arrangements offers any particular advantage in $(L/D)_{max}$ performance, neglecting for now practical considerations such as trim and stability.

Experimental results taken from references 23 and 24, which show the maximum attainable performance obtained from a number of idealized-shape families, are presented in figure 17. In this figure, $(L/D)_{max}$ results are shown as a function of the volume parameter which exerts a large influence on maximum lift-drag-ratio characteristics. The probable range of volume parameters for HCV design is from about 0.14 to 0.24. In this range it is apparent that no one shape family has clearly superior performance and that blended wing-bodies are competitive with discrete wing-body types. At the higher end of the range, slender lifting bodies are also competitive; however, in order to obtain the $(L/D)_{max}$ values shown, extremely slender half-cone bodies are required.

The discrete wing-body data indicate some small improvement in $(L/D)_{max}$ due to the favorable lift interference from the underslung body on the flat-top configurations; and since the introduction of this concept in reference 25, much detailed experimental work (refs. 26 to 37) has been done with the hope of improving the attainable performance. Experimental results from references 26, 27, 28, 33, and 34 are summarized in figure 18. The largest performance gains are obtained at the lower Mach numbers; and, to capitalize on these potential benefits, the design concept was utilized on the XB-70 airplane. At higher Mach numbers, however, the performance gains decrease rapidly. Investigations were undertaken to explain the behavior; and the results, given in detail in reference 34, indicate that performance gains of these idealized shapes are only obtained under rigid geometric constraints. Since these idealized shapes are not generally adaptable to hypersonic cruise vehicle design, further

investigations of the more practical shapes shown in figure 19 were conducted at Mach 6.8. The experimental results to the left indicate the performance gains possible under idealized configuration conditions (shock-shape wings). The more practical configurations, however, fail to show any interference gains in $(L/D)_{max}$. The shapes tested, however, by no means exhaust the interesting possibilities.

The foregoing data were obtained under the effects of a laminar boundary layer. The results in figure 20, however, indicate that under full-scale flight conditions extensive laminar flow will not occur. At the top of the figure are shown typical Reynolds numbers, based on length, for a full-scale hypersonic cruise vehicle. In the lower part of the figure are shown Reynolds number conditions for the start of transition on cones and flat plates, as obtained from references 38 to 55. At Mach 6 to 8, full-scale Reynolds numbers are seen to be greater than 200×10^6 whereas laminar flow ends at about 5×10^6. Only the first few feet of the aircraft, therefore, will be subject to laminar flow, with turbulent flow dominating most of the remaining surface.

In extrapolating laminar wind-tunnel results to turbulent flight conditions, gross approximations presently have to be made. The method used simply subtracts the low Reynolds number laminar skin-friction drag, which in itself is in doubt, and replaces it with high Reynolds number turbulent values. Component performance and interaction effects on lift and drag due to lift are thus assumed to be the same for turbulent flow as for laminar flow - an extremely doubtful assumption. This method was used to extrapolate the previous results of figure 17 to flight conditions, and these extrapolated results are given in figure 21.

As a result of the lower turbulent skin-friction drag at a Reynolds number of 200×10^6 as compared with the laminar drag at 1.5×10^6, the levels of L/D performance are significantly increased and differences in the performance of different configuration families are more pronounced. It is not known, however, whether these trends actually exist because of the difficulty in obtaining turbulent flow on small models at hypersonic Mach numbers as discussed in paper no. 2 by Braslow, Hicks, and Harris. At lower speeds turbulent flow can be simulated by relatively small roughness strips attached to the models. At high Mach numbers this technique is not satisfactory since the required roughness sizes become so large that extraneous effects are often introduced which are difficult, if not imposssible, to correct for (refs. 56 to 63). This problem presents a major difficulty in the present efforts to study complete configurations.

The provision of stability and control will have an important influence on configuration design. Little experimental data on hypersonic air-breathing configurations exist; but during earlier work on boost-glide vehicles, several design features (shown in fig. 22) were developed which may have application to these cruise vehicles.

Negative camber was found to decrease the trim penalties on $(L/D)_{max}$. (See ref. 64.) A negative-camber feature is illustrated by the upward

deflection of the forward portion of the delta wing. Upward deflection of trailing-edge flaps for trim and a properly blunted and contoured underslung body also provide negative-camber effects. In trailing-edge-flap installations, adverse yaw often occurs when these surfaces are differentially deflected for roll control. This effect can be reduced by sweeping the flap hinge line forward to move the resultant force closer to the vehicle center of gravity (ref. 65).

For directional stability and control, a wedge vertical-tail section can reduce excessive area requirements (ref. 66), and a variable wedge could be included to allow optimum operation over the Mach number range and to reduce base drag at critical transonic conditions. Toed-in wing-tip fins (ref. 64) are a further application of the wedge principle. Decreasing directional stability with angle of attack can be alleviated by rolling out the tip fins (ref. 67).

Drooped wing tips may be useful for improving the performance and directional stability with minimum performance penalty for favorable lift-interference configurations but the adverse roll characteristics of these surfaces must not be overlooked.

Local Flow Problems

A major new problem encountered in the design of hypersonic cruise vehicles is the evaluation of local interference effects which may have an important influence on loads, control effectiveness, and local aerodynamic heating. These areas are far more important for these vehicles than for supersonic transport designs because of the more intense interactions which occur between aircraft components. Actually a large amount of study has been devoted to these local flow problems, and in some areas a reasonably good understanding of the phenomena involved already exists.

Turbulent surface-heating data are available on delta wings at local Mach numbers up to about 5 and on flat plates and slender cones at local Mach numbers up to about 8 (refs. 40 to 44, 51 to 55, and 68 to 70). Typical heating results at a free-stream Mach number of 6.8 are shown in figure 23. For delta wings at wall conditions near adiabatic, turbulent heating is predictable by use of strip theory. For cones the heating rates at low angles of attack are predictable by laminar conical-flow theory and at high angles of attack by laminar cross-flow theory with a large uncertainty occurring in the intermediate angle-of-attack range.

Although these results are encouraging, the status of turbulent surface heating must be improved through additional efforts to better establish wall temperature effects and to obtain delta-wing heating characteristics at higher local Mach numbers. In addition, body shapes having larger volumes which are more representative of hypersonic cruise vehicle designs must be investigated.

In leading-edge heating, a somewhat improved situation exists. As long as the Mach number component normal to the leading edge is larger than about 1.5,

laminar and turbulent heating rates are sufficiently predictable for preliminary design purposes on a smooth leading edge (refs. 71 to 74). The effects on heating of the laps on segmented leading edges discussed previously, however, are presently uncertain.

Shock impingement (refs. 75 to 80) has long been recognized as a source of local heating increases. Latest results, however, indicate that these effects on leading edges are predictable. In figure 24 typical results from reference 80 of local heating along the leading edge show an increase from shock impingement. If local conditions are accounted for, the heating increase is well predicted. Shock impingement also causes premature transition from laminar to turbulent flow. However, the transition Reynolds numbers, based on local conditions, have also been determined. Local heating from shock impingement may also occur on surfaces downstream of the leading edge but is less well understood.

Flow separation poses a problem of predicting flap control effectiveness and high heating rates at boundary-layer reattachment on the deflected controls. In reentry vehicles which are subject to laminar or transitional boundary layers, this is a serious problem. In hypersonic cruise vehicles where turbulent flow dominates, however, the problem is much less severe. At the top of figure 25, the large control deflections (refs. 81 to 85) for which a turbulent boundary layer will separate are compared with the much smaller ones for laminar flow. Since control deflections of this order should not be required under normal flight conditions, turbulent flow separation should not be encountered. Should separation occur, however, realistic predictions of control effectiveness and local heating may be possible because of the smaller area affected by turbulent separation as compared with laminar, as illustrated by the schlieren photographs of the flow over a 40° compression corner.

Contrary to the good understanding in the previous areas, the corner-flow problem is not well understood. It occurs at the junctures of the wing and fuselage, wing and tip fins, and inlet sides and wing. The mechanisms of corner flow are very complex and, in spite of the fact that many detailed investigations have been conducted (refs. 86 to 107), local heating increases are not predictable even on the most basic models. Behavior in an idealized corner is illustrated by the unpublished results recently obtained by P. Calvin Stainback in the Langley Mach 8 variable-density hypersonic tunnel and shown in figure 26(a). The model consists of a two-dimensional 90° corner with one side deflected 5° into the stream. The experimental data show heating rates up to five times the predicted values on the undeflected plate and a 50-percent increase in the deflected-plate values. In three-dimensional flow, similar increases occur as indicated by the data in figure 26(b) for a half-cone—delta-wing configuration, taken from reference 51, where the cone heating rates are double the predicted values. These data were obtained under laminar-boundary-layer conditions. The increases in heating under turbulent conditions at these Mach numbers are unknown.

During the development phase of hypersonic cruise vehicles, a number of configuration concepts will have to be considered; and, since these configurations will be significantly different, this inability to predict corner-flow

local heating will require detailed heating tests on each configuration to obtain representative heating distributions. Investigations of complete configurations have begun, and heat-sensitive-paint test results obtained at Mach 6.8 for one concept are shown in figure 27. Regions of high heating are indicated by the dark areas and high heating from corner-flow phenomena is evident near the junctures of the wing and fuselage and the inlet and wing.

CONFIGURATION CONCEPTS

The previous discussion has attempted to isolate presently known influences on configuration definition from the structural, propulsive, and aerodynamic disciplines. To summarize briefly, a discrete body with low or high wing arrangement and fuselage-mounted vertical tail is preferred from the present structural point of view. Propulsive considerations favor a low wing position with two-dimensional inlets mounted in the wing flow field. Both discrete body-wing and blended body-wing arrangements are aerodynamically competitive.

Within these constraints a number of design concepts are possible and some examples of these are shown in figure 28. The three configurations shown in figure 28(a) are being considered in present analytic trade-off studies. The variable-geometry configuration appears to have the highest gross weight but is attractive because of its superior subsonic loiter and mission abort capabilities. Both the variable-geometry and the fixed-delta-wing configuration utilize high-lift devices at take-off and landing. These devices cannot be included on the blended wing-body design, which does not have a separate horizontal tail, and still maintain trim control; as a result, a larger wing area is required for the blended wing-body.

In the trade-off studies, a lifting-body design was also considered; however, the concept was discarded because the high weight of the retractable wing used only for take-off and landing led to large fuel requirements and the resulting gross weight became prohibitive. The success of the twist and camber concept for the supersonic transport requires that it also be considered in the design of hypersonic vehicles, and efforts are now underway to extend the theoretical work to higher Mach numbers.

The configuration at the top of figure 28(b) follows XB-70 design and attempts to gain favorable interference benefits from the wedge underbody. In providing the necessary interference flow field, the underbody becomes large enough to house the inlet ducts and engines and also to provide part of the hydrogen fuel storage volume. A potentially severe problem area exists, however, in the long length of inlet ducts involved which may lead to excessive structural weight and fuel-cooling requirements. Furthermore, the forward inlet position restricts the usable inlet area in the wing flow field.

Another form of a blended wing-body utilizes the "caret" wing proposed in reference 108. The caret-wing lower surface is derived from simple wedge flow and offers more uniform pressure and less severe heating characteristics than does a conventional delta wing. These advantages may, of course, be offset by

other factors such as increased wing area and loads resulting from the negative dihedral.

The configuration on the lower right of figure 28(b) is one "flying inlet" design concept which results when the inlet is too large to be contained in the wing pressure field. It might be applied to higher acceleration Mach 12 cruise vehicles or lower Mach number launch vehicles.

Efforts are now beginning at Ames and Langley Research Centers to investigate complete-configuration concepts which contain requirements of trim, stability, and other practical considerations. The model under study at Mach 7 at Langley is shown in figure 29. As a start, the model design concept is one used in early trade-off studies (ref. 16). This relatively simple concept will serve to verify existing aerodynamic prediction techniques, establish typical local heating distributions, and provide a base-line configuration with which to compare additional concepts which are planned to be added as the program proceeds.

CONCLUDING REMARKS

The principal efforts of the next decade will involve application of the considerable general knowledge and data which now exist in all areas to the development of complete hypersonic vehicle systems. At the present time the first structural-concept models of cryogenic tankage are being readied for high-temperature testing in ground facilities. The first experimental hypersonic ramjet engines for flight tests are under development by both USAF and NASA. Aerodynamic studies of complete configurations have been started.

In the aerodynamics area, there is a serious handicap in the use of existing wind tunnels to simulate the high Reynolds number turbulent flows of full-scale flight. At the higher Mach numbers, the transition-strip technique used so successfully in the supersonic transport development tends to become ineffective. Extensive efforts to develop usable hypersonic tripping techniques are in progress but no practical solution has as yet emerged. Flight tests of at least one representative large-scale wing-body configuration to determine the detailed aerodynamic and heating behavior with natural fully developed turbulent flows will probably be required to supplement and upgrade the wind-tunnel results. This large-scale aerodynamic flight test could also provide the basis for structural concept development and testing for wing-body arrangements which will be needed in the course of future vehicle development.

APPENDIX

SYMBOLS

A_i	inlet captive area
a/g	acceleration in gravity units
d	diameter of cylindrical leading edge
h	heat-transfer coefficient
L/D	lift-drag ratio
l	length
M	Mach number
N_{St}	Stanton number
$p_{t,2}$	duct total pressure
q	dynamic pressure
R_d	Reynolds number based on diameter
R_l	Reynolds number based on length
R_x	Reynolds number based on distance x
S	total planform area
S_w	total wing area (including portion covered by fuselage)
s	distance from center line along surface to a given point
s_o	distance from center line along surface to leading edge
V	volume
V_f	fuel volume
W_f	fuel weight
W_p	payload weight
W_S	structural weight

W_T	gross take-off weight
X,Y,Z	axis system
x,y,z	distance along X-, Y-, and Z-axis, respectively
α	angle of attack
δ	deflection angle

Subscripts:

fb	flat bottom
fp	flat plate
ft	flat top
max	maximum
∞	free stream

Abbreviations:

F.R.	fuselage fineness ratio
LH_2	liquid hydrogen

REFERENCES

1. Sänger, E.; and Bredt, J. (M. Hamermesh, trans.): A Rocket Drive for Long Range Bombers. Transl. CGD-32, Tech. Inform. Branch, Bur. Aeron., Aug. 1944.

2. Williams, E. P.; Dhanes, L. W.; Huntzicker, J. H.; Lew, R. J.; Lieske, H. A.; Moore, L. L.; and Young, G. B. W.: Long-Range Surface-to-Surface Rocket and Ramjet Missiles – Aerodynamics. U.S. Air Force Project RAND Rept. R-181, The RAND Corp., May 1, 1950.

3. Seiff, Alvin; and Allen, H. Julian: Some Aspects of the Design of Hypersonic Boost-Glide Aircraft. NACA RM A55E26, 1955.

4. Eggers, Alfred J., Jr.; Allen, H. Julian; and Neice, Stanford E.: A Comparative Analysis of the Performance of Long-Range Hypervelocity Vehicles. NACA Rept. 1382, 1958. (Supersedes NACA TN 4046.)

5. Gradecak, V.: A Typical Long Range Hypersonic Rocket Glider and Its Structural Problems. 3rd Symposium on High-Speed Aerodynamics and Structures, Vol. 2, CONVAIR – San Diego, 1958, pp. 243-338.

6. Weber, R. J.: A Survey of Hypersonic-Ramjet Concepts. [Preprint] 875-59, Am. Rocket Soc., June 1959.

7. Frick, C. W.; and Strand, T.: Recoverable Air-Breathing Boosters - Analysis of Their Potentialities. Aerospace Eng., vol. 20, no. 2, Feb. 1961, pp. 22-23, 66-70.

8. Lane, R. J.: Recoverable Air-Breathing Boosters for Space Vehicles. J. Roy. Aeron. Soc., vol. 66, no. 618, June 1962, pp. 371-386.

9. Watton, Alan: Aerospaceplane – An Advanced System Planning Study. ASD-TDR-63-390, U.S. Air Force, Sept. 1963.

10. Tinnan, Leonard M.: Reusable Launch Systems. Astronautics, vol. 8, no. 1, Jan. 1963, pp. 50-56.

11. Jarlett, F. E.: Aerospaceplane Payload and Potential. Trans. Eighth Symposium on Ballistic Missile and Space Technology, vol. V, U.S. Air Force and Aerospace Corp., Oct. 1963, pp. 243-303. (Available from DDC as AD 346-902.)

12. Knip, Gerald, Jr.; and Allen, John L.: Analysis of Booster Systems With a Recoverable Hypersonic Airplane First Stage. AIAA Paper No. 64-543, May 1964.

13. Peoples, P. L.; Zeck, H.; Edmonds, D. S.; and Omoth, M. J.: Performance and Cost Analysis of Advanced Rocket and Airbreathing Launch Systems. AIAA/NASA Third Manned Space Flight Meeting, CP-10, Am. Inst. Aeron. Astronaut., Nov. 1964, pp. 339-352.

14. Petersen, Richard H.; Gregory, Thomas J.; and Smith, Cynthia L.: Some Comparisons of Turboramjet-Powered Hypersonic Aircraft for Cruise and Boost Missions. AIAA Paper No. 65-759, Nov. 1965.

15. Watton, Alan: Recent Air-Breathing Launch Vehicle Studies and Their Propulsion Implications. 65SES-1246, RTD, U.S. Air Force, June 15, 1965.

16. Gregory, Thomas J.; Petersen, Richard H.; and Wyss, John A.: Performance Trade-Offs and Research Problems for Hypersonic Transports. Paper No. 64-605, Am. Inst. Aeron. Astronaut., Aug. 1964.

17. Weber, Richard J.: Propulsion for Hypersonic Transport Aircraft. Proceedings of the 4th Congress of the International Council of the Aeronautical Sciences, Robert R. Dexter, ed., Spartan Books, Inc., 1965, pp. 977-999.

18. Manning, Charles R., Jr.; Royster, Dick M.; and Braski, David N.: An Investigation of a New Nickel Alloy Strengthened by Dispersed Thoria. NASA TN D-1944, 1963.

19. Lisagor, W. Barry; and Stein, Bland A.: A Study of Several Oxidation-Resistant Coatings on Cb-10Ti-5Zr Alloy Sheet at 2000° F, 2400° F, and 2700° F (1365° K, 1590° K, and 1755° K). NASA TN D-3275, 1966.

20. Scott, Russell Burton: Cryogenic Engineering. D. Van Nostrand Co., Inc., 1959.

21. Jackson, L. Robert; Davis, John G., Jr.; and Wichorek, Gregory R.: Structural Concepts for Hydrogen-Fueled Hypersonic Airplanes. NASA TN D-3162, 1966.

22. Jackson, Charlie M., Jr.: Estimation of Flight Performance With Closed-Form Approximations to the Equations of Motion. NASA TR R-228, 1966.

23. Becker, John V.: Studies of High Lift/Drag Ratio Hypersonic Configurations. Proceedings of the 4th Congress of the International Council of the Aeronautical Sciences, Robert R. Dexter, ed., Spartan Books, Inc., 1965, pp. 877-910.

24. Penland, Jim A.: Maximum Lift-Drag-Ratio Characteristics of Rectangular and Delta Wings at Mach 6.9. NASA TN D-2925, 1965.

25. Eggers, A. J., Jr.; and Syvertson, Clarence A.: Aircraft Configurations Developing High Lift-Drag Ratios at High Supersonic Speeds. NACA RM A55L05, 1956.

26. Syvertson, Clarence A.; Gloria, Hermilo R.; and Sarabia, Michael F.: Aerodynamic Performance and Static Stability and Control of Flat-Top Hypersonic Gliders at Mach Numbers From 0.6 to 18. NACA RM A58G17, 1958.

27. Syvertson, Clarence A.; Wong, Thomas J.; and Gloria, Hermilo, R.: Additional Experiments With Flat-Top Wing-Body Combinations at High Supersonic Speeds. NACA RM A56I11, 1957.

28. Armstrong, William O.; and Ladson, Charles L. (With Appendix by Donald L. Baradell and Thomas A. Blackstock): Effects of Variation in Body Orientation and Wing and Body Geometry on Lift-Drag Characteristics of a Series of Wing-Body Combinations at Mach Numbers From 3 to 18. NASA TM X-73, 1959.

29. McLellan, Charles H.; and Dunning, Robert W.: Factors Affecting the Maximum Lift-Drag Ratio at High Supersonic Speeds. NACA RM L55L20a, 1956.

30. McLellan, Charles H.; and Ladson, Charles L.: A Summary of the Aerodynamic Performance of Hypersonic Gliders. NASA TM X-237, 1960.

31. Mead, Harold R.; Koch, Frank; and Hartofilis, Stavros A.: Theoretical Prediction of Pressures in Hypersonic Flow With Special Reference to Configurations Having Attached Leading-Edge Shock. ASD TR 61-60, U.S. Air Force. Part II. Experimental Pressure Measurements at Mach 5 and 8, May 1962. Part III. Experimental Measurements of Forces at Mach 8 and Pressures at Mach 21, Oct. 1962. (Available from ASTIA as 291 219.)

32. Geiger, Richard E.: Experimental Lift and Drag of a Series of Glide Configurations at Mach Numbers 12.6 and 17.5. J. Aerospace Sci., vol. 29, no. 4, Apr. 1962, pp. 410-419.

33. Johnston, Patrick J.; Snyder, Curtis D.; and Witcofski, Robert D.: Maximum Lift-Drag Ratios of Delta-Wing—Half-Cone Combinations at a Mach Number of 20 in Helium. NASA TN D-2762, 1965.

34. Fetterman, David E.: Favorable Interference Effects on Maximum Lift-Drag Ratios of Half-Cone Delta-Wing Configurations at Mach 6.86. NASA TN D-2942, 1965.

35. Fetterman, David E.; Henderson, Arthur, Jr.; Bertram, Mitchel H.; and Johnston, Patrick J.: Studies Relating to the Attainment of High Lift-Drag Ratios at Hypersonic Speeds. NASA TN D-2956, 1965.

36. Small, William J.; and Bertram, Mitchel H.: Effect of Geometric Modifications on the Maximum Lift-Drag Ratios of Slender Wing-Body Configurations at Hypersonic Speeds. NASA TN D-3276, 1966.

37. Whitehead, Allen H., Jr.: Effect of Body Cross Section and Width-Height Ratio on Performance of Bodies and Delta-Wing—Body Combinations at Mach 6.9. NASA TN D-2886, 1966.

38. Bertram, Mitchel H.: Exploratory Investigation of Boundary-Layer Transition on a Hollow Cylinder at a Mach Number of 6.9. NACA Rept. 1313, 1957. (Supersedes NACA TN 3546.)

39. Potter, J. Leith; and Whitfield, Jack D.: Effects of Unit Reynolds Number, Nose Bluntness, and Roughness on Boundary Layer Transition. AEDC-TR-60-5, U.S. Air Force, Mar. 1960.

40. Zakkay, Victor; and Callahan, Clifton J.: Laminar, Transitional, and Turbulent Heat Transfer to a Cone-Cylinder-Flare Body at Mach 8.0. J. Aerospace Sci., vol. 29, no. 12, Dec. 1962, pp. 1403-1413, 1420.

41. Deem, Ralph E.; and Murphy, James S.: Flat Plate Boundary Layer Transition at Hypersonic Speeds. AIAA Paper No. 65-128, Jan. 1965.

42. Sanator, R. J.; DeCarlo, J. P.; and Torrillo, D. T.: Hypersonic Boundary-Layer Transition Data for a Cold-Wall Slender Cone. AIAA J. (Tech. Notes), vol. 3, no. 4, Apr. 1965, pp. 758-760.

43. Bertram, Mitchel H.; and Neal, Luther, Jr.: Recent Experiments in Hypersonic Turbulent Boundary Layers. Presented at the AGARD Specialists Meeting on Recent Developments in Boundary-Layer Research (Naples, Italy), May 10-14, 1965.

44. Richards, B. E.; and Stollery, J. L.: Transition Reversal on a Flat Plate at Hypersonic Speeds. Recent Developments in Boundary Layer Research, AGARDograph 97, May 1965, pp. 477-501.

45. McCauley, W. D.; Saydah, A.; and Bueche, J.: The Effect of Controlled Three Dimensional Roughness on Hypersonic Laminar Boundary Layer Transition. AIAA Paper No. 66-26, Jan. 1966.

46. Henderson, A.; Rogallo, R. S.; Woods, W. C.; and Spitzer, C. R.: Exploratory Hypersonic Boundary-Layer Transition Studies. AIAA J. (Tech. Notes), vol. 3, no. 7, July 1965, pp. 1363-1364.

47. Fischer, W. W.; and Norris, R. H.: Supersonic Convective Heat-Transfer Correlation From Skin-Temperature Measurements on a V-2 Rocket in Flight. Trans. ASME, vol. 71, no. 5, July 1949, pp. 457-469.

48. Sternberg, Joseph: A Free-Flight Investigation of the Possibility of High Reynolds Number Supersonic Laminar Boundary Layers. J. Aeron. Sci., vol. 19, no. 11, Nov. 1952, pp. 721-733.

49. Jedlicka, James R.; Wilkins, Max E.; and Seiff, Alvin: Experimental Determination of Boundary-Layer Transition on a Body of Revolution at M = 3.5. NACA TN 3342, 1954.

50. Stetson, Kenneth F.: Boundary-Layer Transition on Blunt Bodies With Highly Cooled Boundary Layers. J. Aero/Space Sci., vol. 27, no. 2, Feb. 1960, pp. 81-91.

51. Dunavant, James C.: Heat Transfer to a Delta-Wing—Half-Cone Combination at Mach Numbers of 7 and 10. NASA TN D-2199, 1964.

52. Crawford, Davis H.: Investigation of the Flow Over a Spiked-Nose Hemisphere-Cylinder at a Mach Number of 6.8. NASA TN D-118, 1959.

53. Jackson, Mary W.; Czarnecki, K. R.; and Monta, William J.: Turbulent Skin Friction at High Reynolds Numbers and Low Supersonic Velocities. NASA TN D-2687, 1965.

54. Moore, D. R.; and Harkness, J.: Experimental Investigations of the Compressible Turbulent Boundary Layer at Very High Reynolds Numbers. AIAA J., vol. 3, no. 4, Apr. 1965, pp. 631-638.

55. Monta, William J.; and Allen, Jerry M.: Local Turbulent Skin-Friction Measurements on a Flat Plate at Mach Numbers From 2.5 to 4.5 and Reynolds Numbers up to 69×10^6. NASA TN D-2896, 1965.

56. Braslow, Albert L.; and Knox, Eugene C.: Simplified Method for Determination of Critical Height of Distributed Roughness Particles for Boundary-Layer Transition at Mach Numbers From 0 to 5. NACA TN 4363, 1958.

57. Smith, A. M. O.; and Clutter, Darwin W.: The Smallest Height of Roughness Capable of Affecting Boundary-Layer Transition. J. Aero/Space Sci., vol. 26, no. 4, Apr. 1959, pp. 229-245, 256.

58. Braslow, Albert L.: Review of the Effect of Distributed Surface Roughness on Boundary-Layer Transition. AGARD Rept. 254, Apr. 1960.

59. Van Driest, E. R.; and Blumer, C. B.: Effect of Roughness on Transition in Supersonic Flow. AGARD Rept. 255, Apr. 1960.

60. Von Doenhoff, Albert E.; and Braslow, Albert L.: The Effect of Distributed Surface Roughness on Laminar Flow. Boundary Layer and Flow Control, Vol. 2, G. V. Lachmann, ed., Pergamon Press, 1961, pp. 657-681.

61. Korkegi, Robert H.: Transition Studies and Skin-Friction Measurements on an Insulated Flat Plate at a Mach Number of 5.8. J. Aeron. Sci., vol. 23, no. 2, Feb. 1956, pp. 97-107, 192.

62. Sterrett, James R.; and Holloway, Paul F.: Effects of Controlled Roughness on Boundary-Layer Transition at a Mach Number of 6.0. AIAA J. (Tech. Notes), vol. 1, no. 8, Aug. 1963, pp. 1951-1953.

63. Holloway, Paul F.; and Sterrett, James R.: Effect of Controlled Surface Roughness on Boundary-Layer Transition and Heat Transfer at Mach Numbers of 4.8 and 6.0. NASA TN D-2054, 1964.

64. Rainey, Robert W.: Static Stability and Control of Hypersonic Gliders. NACA RM L58E12a, 1958.

65. Rainey, Robert W.: Summary of an Advanced Manned Lifting Entry Vehicle Study. NASA TM X-1159, 1965.

66. McLellan, Charles H.: A Method for Increasing the Effectiveness of Stabilizing Surfaces at High Supersonic Mach Numbers. NACA RM L54F21, 1954.

67. Rainey, Robert W.; and Close, William H.: Studies of Stability and Control of Winged Reentry Configurations. NASA TM X-327, 1960.

68. Nagel, A. L.; Fitzsimmons, H. D.; and Doyle, L. B.: Analysis of Hypersonic Pressure and Heat Transfer Tests on Delta Wings With Laminar and Turbulent Boundary Layers. D2-84299-1 (Contract No. NAS1-4301), The Boeing Co.

69. Stallings, Robert L., Jr.; Burbank, Paige B.; and Howell, Dorothy T.: Heat-Transfer and Pressure Measurements on Delta Wings at Mach Numbers of 3.51 and 4.65 and Angles of Attack From -45° to 45°. NASA TN D-2387, 1964.

70. Dunavant, James C.: Investigation of Heat Transfer and Pressures on Highly Swept Flat and Dihedraled Delta Wings at Mach Numbers of 6.8 and 9.6 and Angles of Attack to 90°. NASA TM X-688, 1962.

71. Everhart, Philip E.; and Dunavant, James C.: Heat-Transfer Distribution on 70° Swept Slab Delta Wings at a Mach Number of 9.86 and Angles of Attack up to 90°. NASA TN D-2302, 1964.

72. Whitehead, Allen H., Jr.; and Dunavant, James C.: A Study of Pressure and Heat Transfer Over an 80° Sweep Slab Delta Wing in Hypersonic Flow. NASA TN D-2708, 1965.

73. Bertram, Mitchel H.; and Everhart, Philip E.: An Experimental Study of the Pressure and Heat-Transfer Distribution on a 70° Sweep Slab Delta Wing in Hypersonic Flow. NASA TR R-153, 1963.

74. Beckwith, Ivan E.; and Gallagher, James J.: Local Heat Transfer and Recovery Temperatures on a Yawed Cylinder at a Mach Number of 4.15 and High Reynolds Numbers. NASA TR R-104, 1961. (Supersedes NASA MEMO 2-27-59L.)

75. Newlander, Robert A.: Effect of Shock Impingement on the Distribution of Heat-Transfer Coefficients on a Right Circular Cylinder at Mach Numbers of 2.65, 3.51, and 4.44. NASA TN D-642, 1961.

76. Carter, Howard S.; and Carr, Robert E.: Free-Flight Investigation of Heat Transfer to an Unswept Cylinder Subjected to an Incident Shock and Flow Interference From an Upstream Body at Mach Numbers up to 5.50. NASA TN D-988, 1961.

77. Beckwith, Ivan E.: Experimental Investigation of Heat Transfer and Pressures on a Swept Cylinder in the Vicinity of its Intersection With a Wedge and Flat Plate at Mach Number 4.15 and High Reynolds Numbers. NASA TN D-2020, 1964.

78. Knox, E. C.: Measurements of Shock-Impingement Effects on the Heat-Transfer and Pressure Distributions on a Hemicylinder Model at Mach Number 19. AEDC-TR-65-245, U.S. Air Force. Nov. 1965.

79. Siler, L. G.; and Deskins, H. E.: Effect of Shock Impingement on the Heat-Transfer and Pressure Distributions on a Cylindrical-Leading-Edge Model at Mach Number 19. AEDC-TDR-64-228, U.S. Air Force, Nov. 1964.

80. Bushnell, Dennis M.: Interference Heating on a Swept Cylinder in Region of Intersection With a Wedge at Mach Number 8. NASA TN D-3094, 1965.

81. Chapman, Dean R.; Kuehn, Donald M.; and Larson, Howard K.: Investigation of Separated Flows in Supersonic and Subsonic Streams With Emphasis on the Effect of Transition. NACA Rept. 1356, 1958.

82. Kuehn, Donald M.: Turbulent Boundary-Layer Separation Induced by Flares on Cylinders at Zero Angle of Attack. NASA TR R-117, 1961.

83. Sterrett, James R.; and Emery, James C.: Experimental Separation Studies for Two-Dimensional Wedges and Curved Surfaces at Mach Numbers of 4.8 to 6.2. NASA TN D-1014, 1962.

84. Kuehn, Donald M.: Experimental Investigation of the Pressure Rise Required for the Incipient Separation of Turbulent Boundary Layers in Two-Dimensional Supersonic Flow. NASA MEMO 1-21-59A, 1959.

85. Holloway, Paul F.; Sterrett, James R.; and Creekmore, Helen S.: An Investigation of Heat Transfer Within Regions of Separated Flow at a Mach Number of 6.0. NASA TN D-3074, 1965.

86. Snow, R. M.: Aerodynamics of Thin Quadrilateral Wings at Supersonic Speeds. Quart. Appl. Math., vol. V, no. 4, Jan. 1948, pp. 417-428.

87. Hains, Franklin D.: Supersonic Flow Near the Junction of Two Wedges. J. Aero/Space Sci. (Readers' Forum), vol. 25, no. 8, Aug. 1958, pp. 530-531.

88. Wallace, James; and Clarke, Joseph H.: Uniformly Valid Second-Order Solution for Supersonic Flow Over Cruciform Surfaces. AIAA J., vol. 1, no. 1, Jan. 1963, pp. 179-185.

89. Loiziansky, L. G.: Interference of Boundary Layers. No. 249, Trans. Central Aero-Hydrodynamical Inst. (Moscow), 1936.

90. Loitsianskii, L. G.; and Bolshakov, V. P.: On Motion of Fluid in Boundary Layer Near Line of Intersection of Two Flows. NACA TM 1308, 1951.

91. Carrier, G. F.: The Boundary Layer in a Corner. Quart. Appl. Math., vol. IV, no. 4, Jan. 1947, pp. 367-370.

92. Dowdell, Rodger Birtwell: Corner Boundary Layer. M.S. Thesis, Brown Univ., 1952.

93. Oman, Richard A.: The Three-Dimensional Laminar Boundary Layer Along a Corner. Tech. Rept. No. 1 (Contract No. DA-19-020-ORD-4538), M.I.T., Jan. 1959. (Available from ASTIA as AD 211 216.)

94. Kemp, Nelson Harvey: The Laminar Three-Dimensional Boundary Layer and a Study of the Flow Past a Side Edge. M. Aero. Eng. Thesis, Cornell Univ., June 1951. (Available from ASTIA as AD 45462.)

95. Levy, Richard H.: The Boundary Layer in a Corner. Contract AF 49(638)-465, Dept. Aeron. Eng., Princeton Univ., Nov. 1959.

96. Cheng, Sin-I; and Levy, Richard H.: The Boundary Layer in a Corner. Rept. No. 485 (AFOSR TN 59-1165), Princeton Univ., Nov. 1959.

97. Krzywoblocki, M. Z.: On the Boundary Layer in a Corner by Use of the Relaxation Method. Ganita (Lucknow, India), vol. 7, no. 2, Dec. 1956, pp. 76-112.

98. Bloom, Martin H.; and Rubin, Stanley: High-Speed Viscous Corner Flow. J. Aerospace Sci., vol. 28, no. 2, Feb. 1961, pp. 145-157.

99. Stainback, P. Calvin: An Experimental Investigation at a Mach Number of 4.95 of Flow in the Vicinity of a 90° Interior Corner Alined With the Free-Stream Velocity. NASA TN D-184, 1960.

100. Stainback, P. Calvin: Heat-Transfer Measurements at a Mach Number of 8 in the Vicinity of a 90° Interior Corner Alined With the Free-Stream Velocity. NASA TN D-2417, 1964.

101. Galowin, Lawrence: Heat Transfer Correlations for the 90° Corner Interference Effects on Fin-Flat Plate Model at a Mach Number of 8. Tech. Rept. No. 207 (Contract No. AF 33(616)-6692), Gen. Appl. Sci. Lab., Inc., Feb. 8, 1961.

102. Bogdonoff, S. M.; and Vas, I. E.: A Preliminary Investigation of the Flow in a 90° Corner at Hypersonic Speeds. Part I – Flat Plates With Thin Leading Edges at Zero Angle of Attack. D143-978-013 (ARDC TR 57-202, AD 150 023), Bell Aircraft Corp., Dec. 20, 1957.

103. Rhudy, J. P.; Miers, R. S.; and Rippey, J. O.: Pressure Distribution and Heat Transfer Tests on Two Fin-Flat Plate Interference Models and Several Blunt Leading Edge Delta Wing Models. AEDC-TN-60-168, U.S. Air Force, Sept. 1960.

104. Miller, D. S.; Hijman, R.; Redeker, E.; Janssen, W. C.; and Mullen, C. R.: A Study of Shock Impingements on Boundary Layers at Mach 16. Proc. 1962 Heat Transfer and Fluid Mech. Inst., F. Edward Ehlers, James J. Kauzlarich, Charles A. Sleicher, Jr., and Robert E. Street, eds., Stanford Univ. Press, 1962, pp. 255-278.

105. Caldwell, A. L.; Haugseth, E. G.; and Miller, D. S.: The Influence of Aerodynamic Interference Heating on Directional Stability Problems of Hypersonic Vehicles. Paper 63-3, Inst. Aerospace Sci., Jan. 1963.

106. Jones, Robert A.: Heat-Transfer and Pressure Investigation of a Fin-Plate Interference Model at a Mach Number of 6. NASA TN D-2028, 1964.

107. Charwat, A. F.; and Redekopp, L. G.: Supersonic Interference Flow Along the Corner of Intersecting Wedges. AIAA Paper 66-128, Jan. 1966.

108. Townsend, L. H.: On Lifting Bodies Which Contain Two-Dimensional Supersonic Flows. Rept. No. Aero. 2675, Brit. R.A.E., Aug. 1963.

TABLE I

TYPICAL RESULTS FROM NASA CRUISE VEHICLE STUDIES

ITEM	SST STUDY	HCV STUDY
M_∞	3	6
RANGE, N.Mi.	3500	5500
W_T, LB	500000	500000
FUEL	JP	LH_2
W_p/W_T	0.08	0.09
W_f/W_T	0.50	0.38
V_f, FT^3	4900	43500
W_S/W_T	0.27	0.36
F. R.	22 TO 24	12 TO 14
$(L/D)_{max}$	8 TO 9	4.5 TO 5.0
W_T/S_w	55 TO 100	45 TO 120

FLIGHT-PROFILE CONSTRAINTS

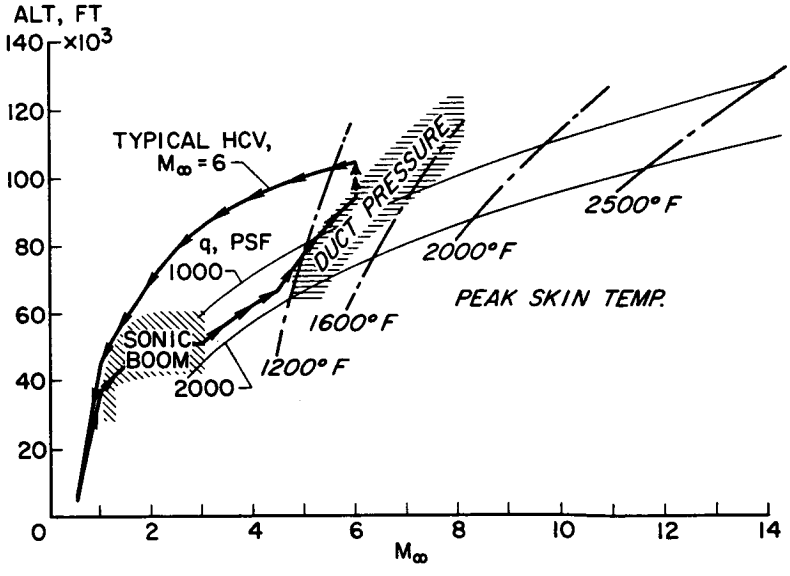

Figure 1

SIZE COMPARISON BETWEEN HCV AND SST

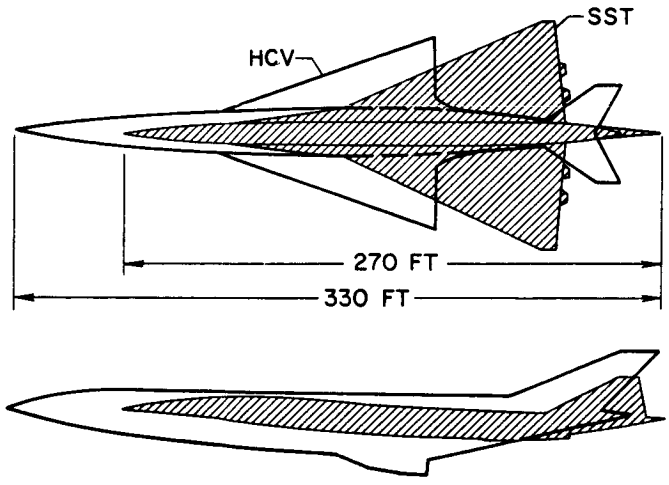

Figure 2

EXAMPLE OF HCV STRUCTURAL ARRANGEMENT

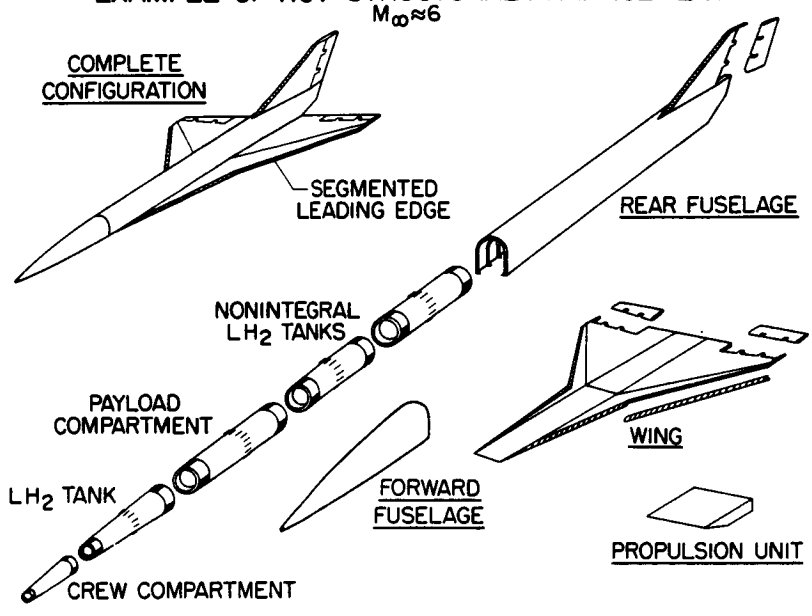

Figure 3

A NONINSULATED WING STRUCTURAL CONCEPT
$M_\infty \approx 6$

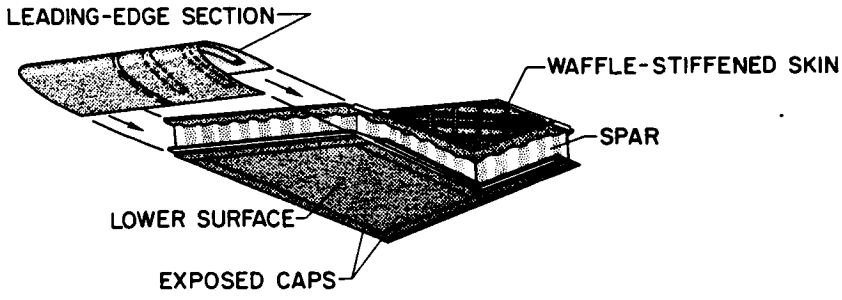

Figure 4

AN INSULATED WING STRUCTURAL CONCEPT
$M_\infty \approx 12$

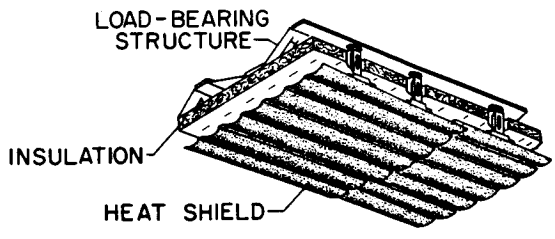

Figure 5

NONINTEGRAL TANKAGE STRUCTURES

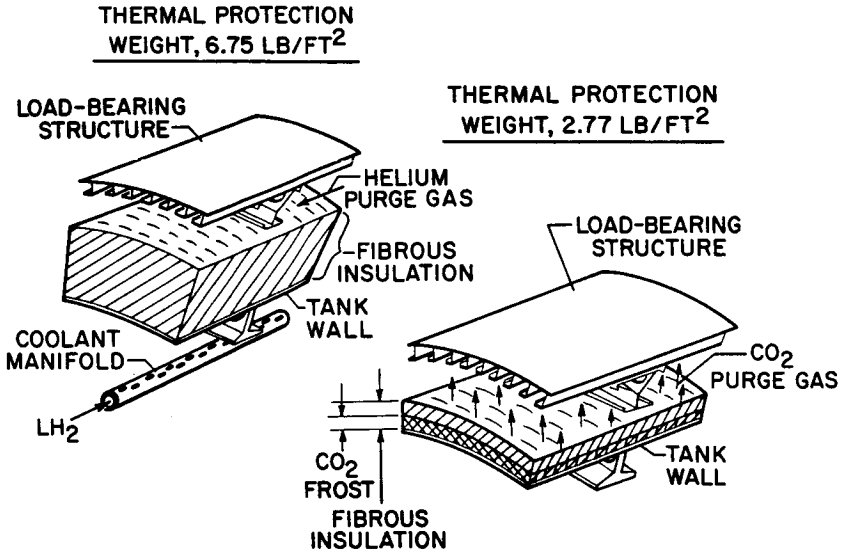

Figure 6

HOT STRUCTURAL MODEL WITH NONINTEGRAL TANKAGE AND CO_2 PURGE SYSTEM

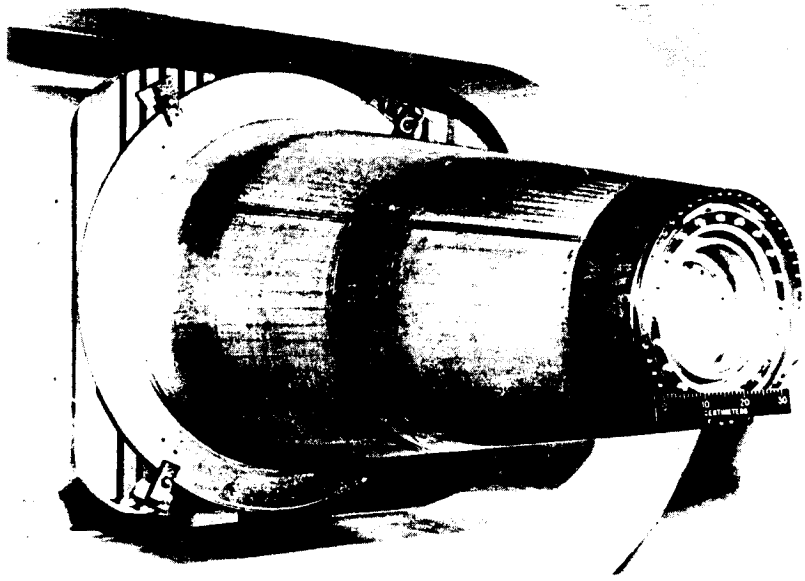

Figure 7 L-65-8668

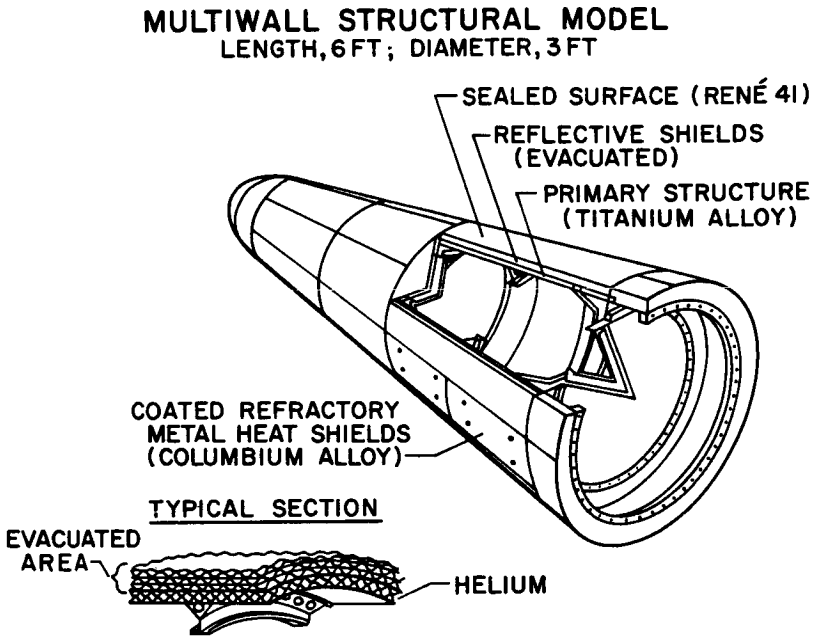

Figure 8

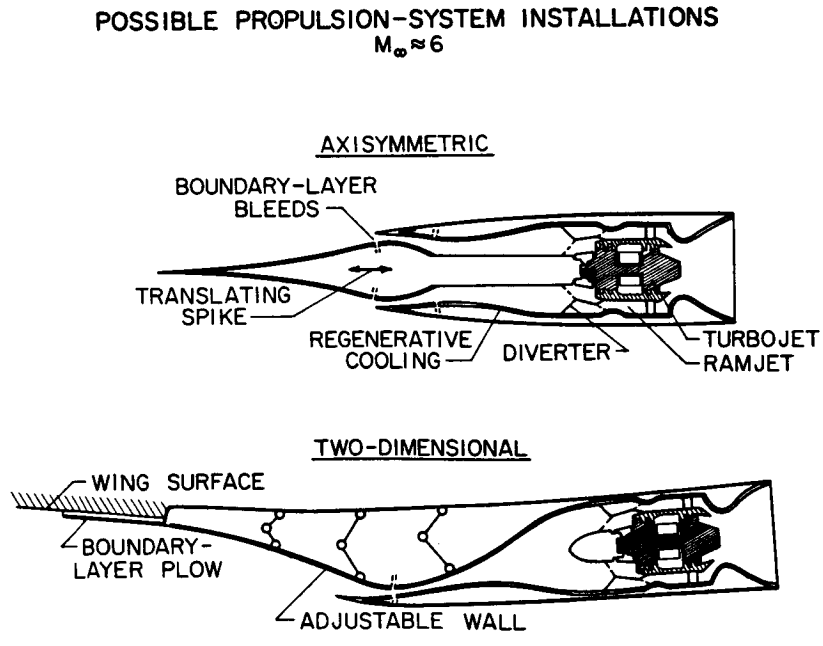

Figure 9

REPRESENTATIVE ACCELERATION FLIGHT PATH

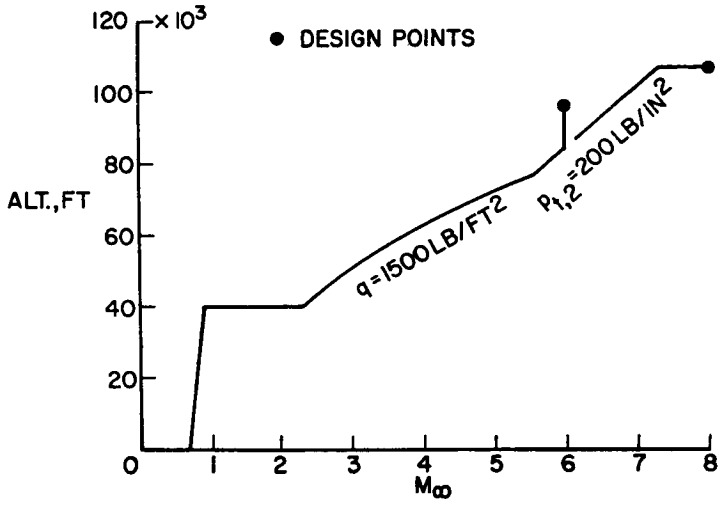

Figure 10

AERODYNAMIC CHARACTERISTICS DURING ACCELERATING FLIGHT

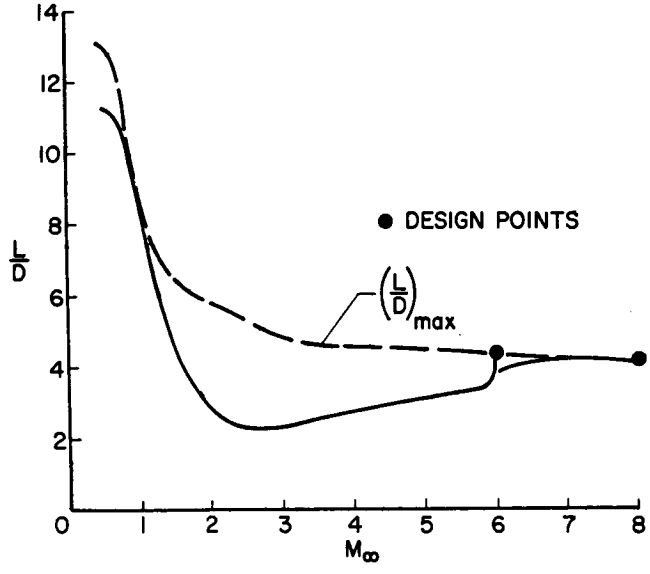

Figure 11

REPRESENTATIVE ACCELERATION CHARACTERISTICS

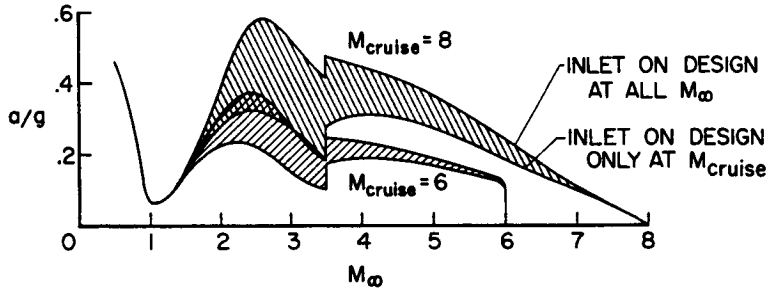

Figure 12

FACTORS AFFECTING INLET SIZE AND LOCATION

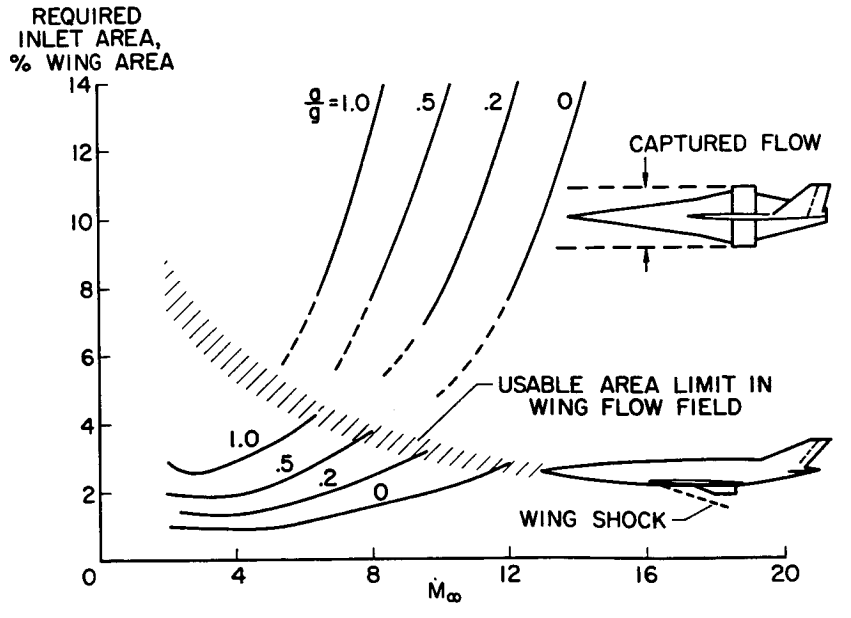

Figure 13

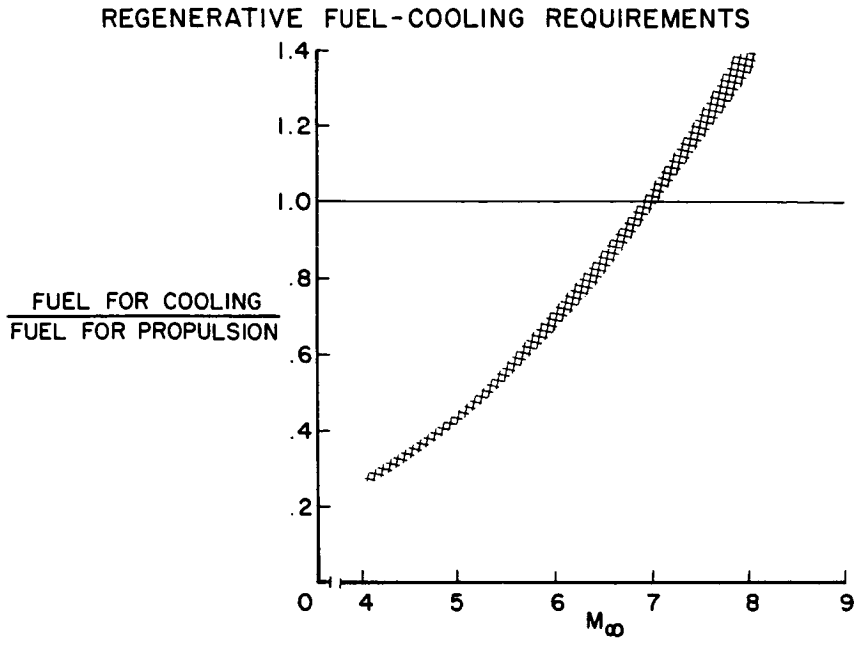

Figure 14

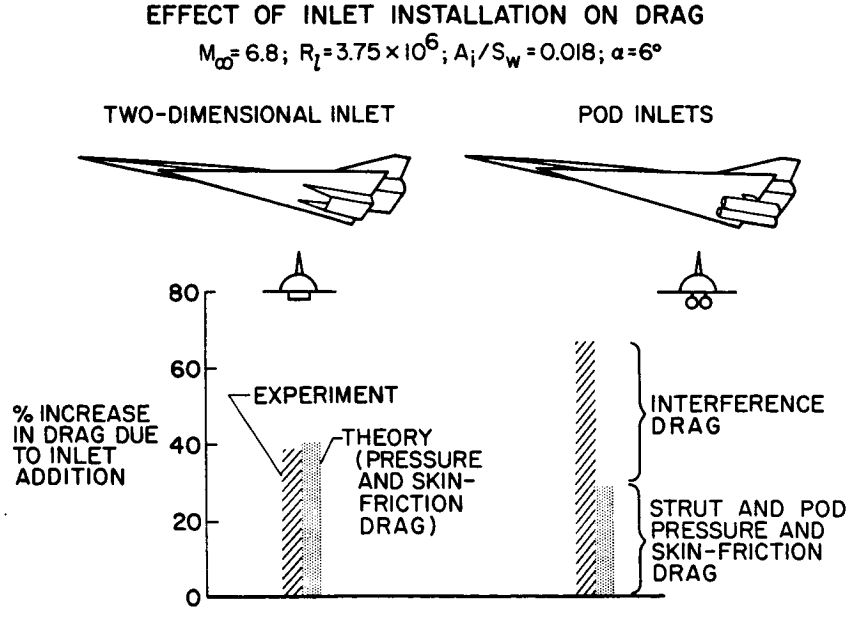

Figure 15

INLET INSTALLATION OIL-FLOW PATTERNS

$M_\infty = 6.8$; $A_i/S_w = 0.018$

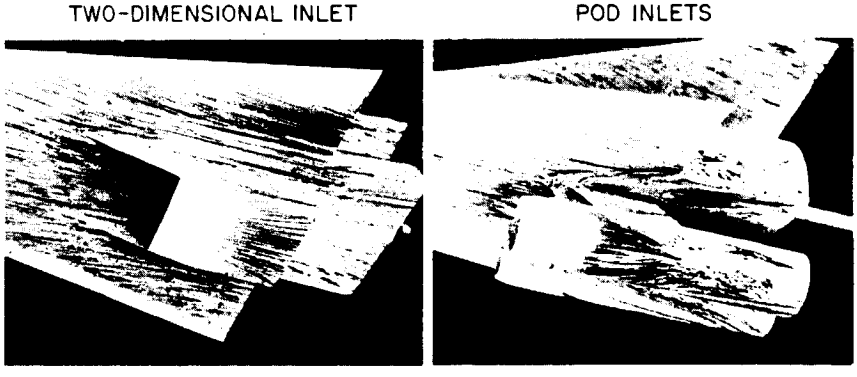

Figure 16 L-2697-24

PERFORMANCE OF BASIC CONFIGURATION CONCEPTS MEASURED IN WIND TUNNEL

$M_\infty = 6.8$; $R_l = 1.5 \times 10^6$

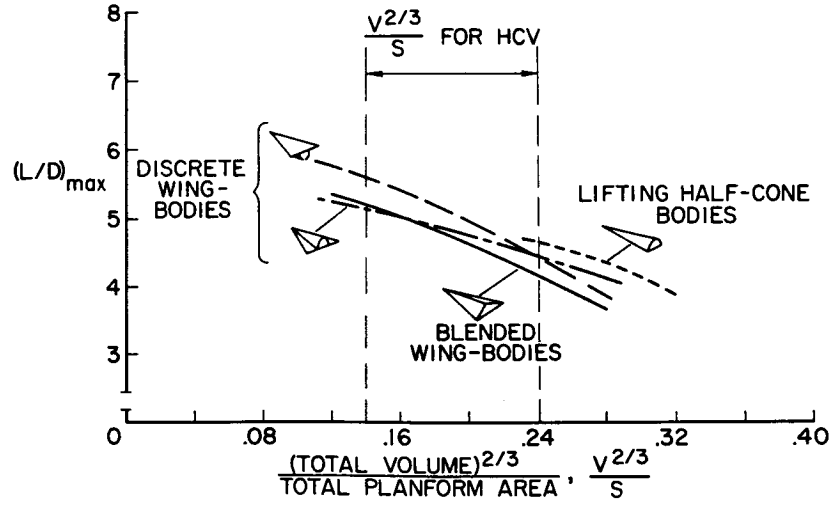

Figure 17

WING-BODY INTERFERENCE EFFECTS ON PERFORMANCE

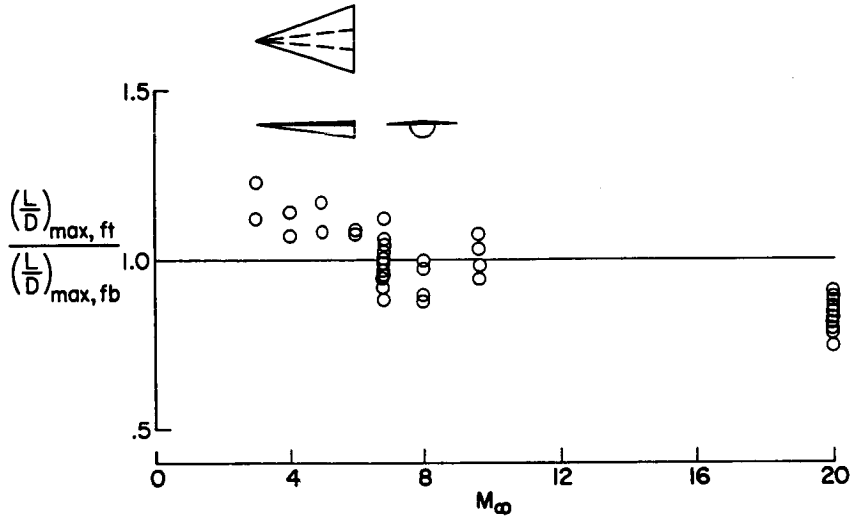

Figure 18

BASIC CONFIGURATION EFFECTS ON UNTRIMMED PERFORMANCE

$M_\infty = 6.8$; $R_l = 3.9 \times 10^6$; BODY VOLUME CONSTANT

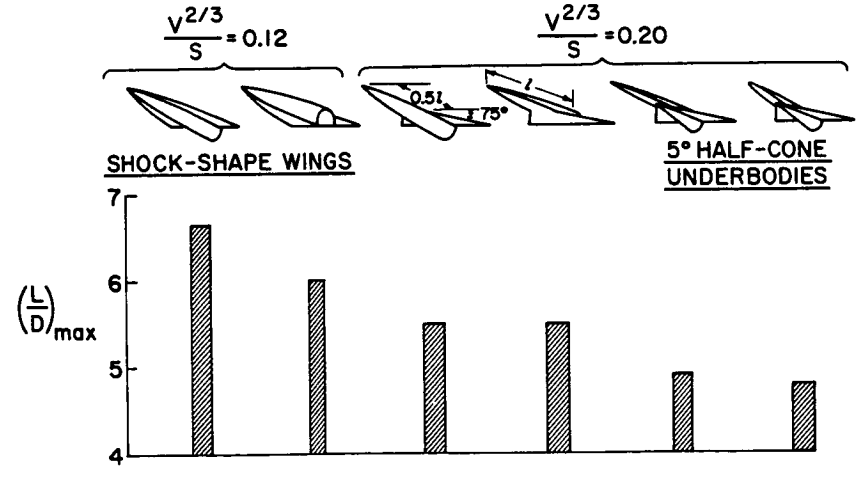

Figure 19

COMPARISON OF TRANSITION AND FULL-SCALE REYNOLDS NUMBER

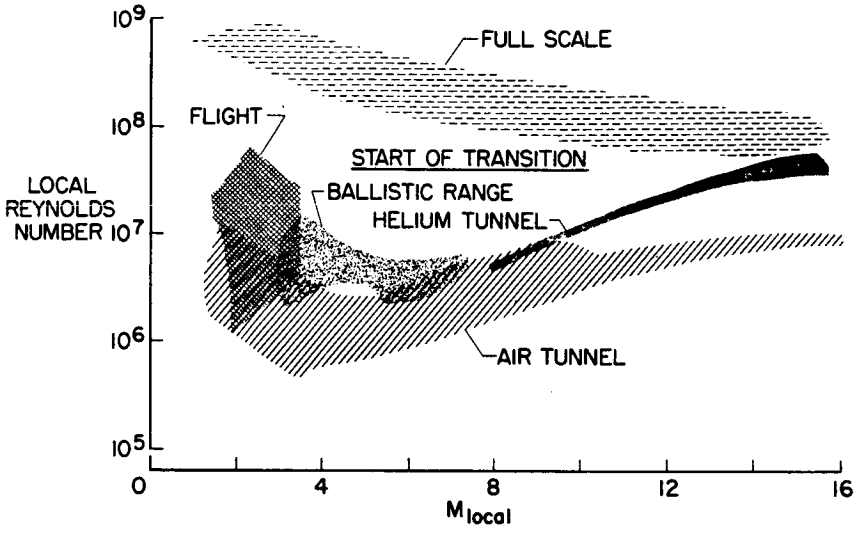

Figure 20

PERFORMANCE OF BASIC CONFIGURATION CONCEPTS EXTRAPOLATED TO FLIGHT CONDITIONS

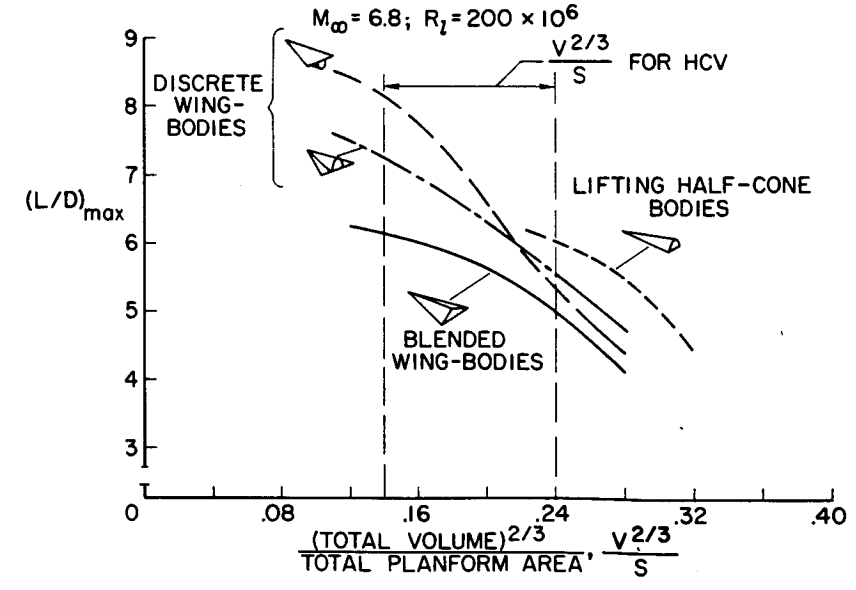

Figure 21

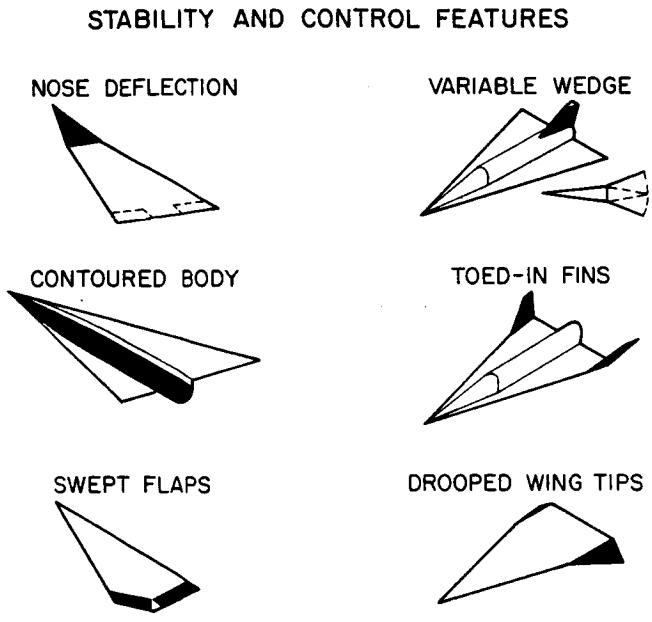

Figure 22

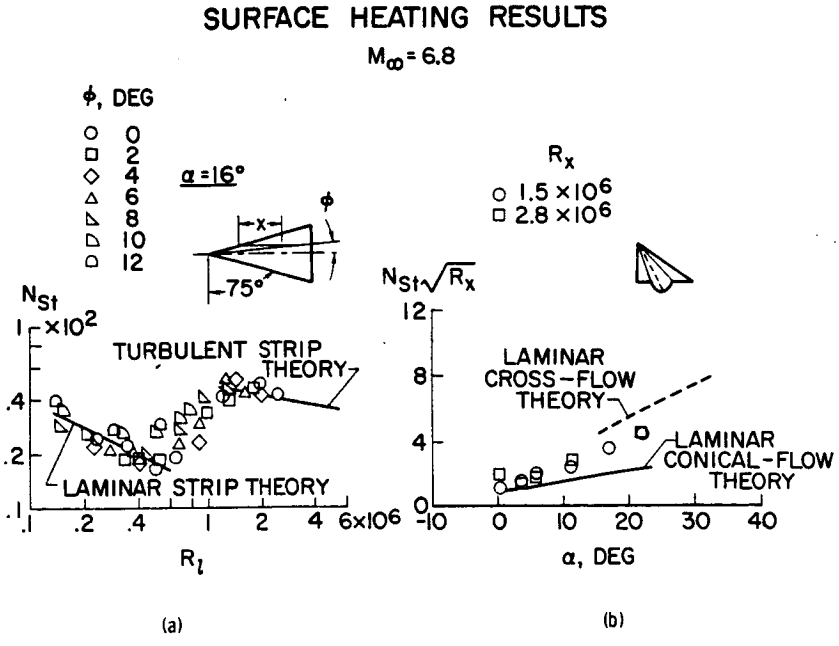

Figure 23

TYPICAL SHOCK-IMPINGEMENT RESULTS

$M_\infty \approx 8$; $R_d = 0.25 \times 10^6$

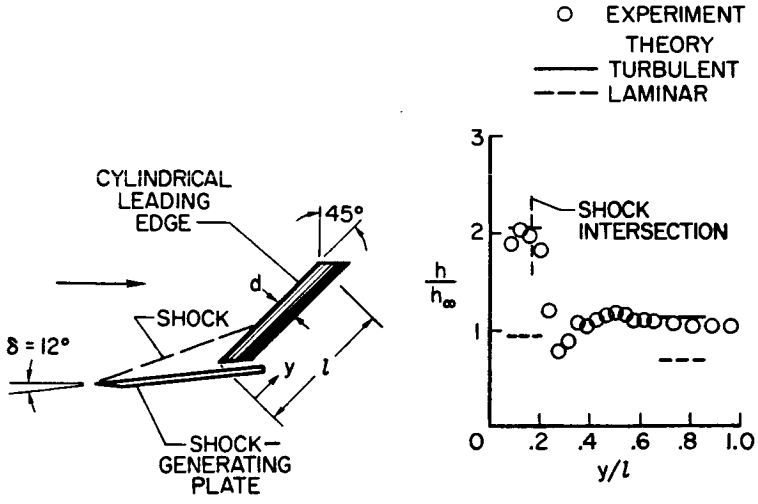

Figure 24

TURBULENT FLOW SEPARATION

MAXIMUM FLOW DEFLECTION WITH NO SEPARATION

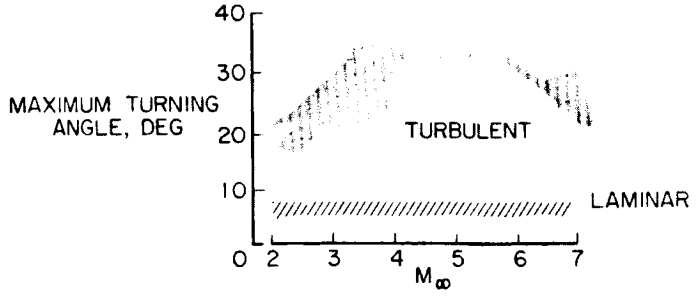

SCHLIEREN RESULTS AT $M_\infty = 6.8$

Figure 25

L-2697-20

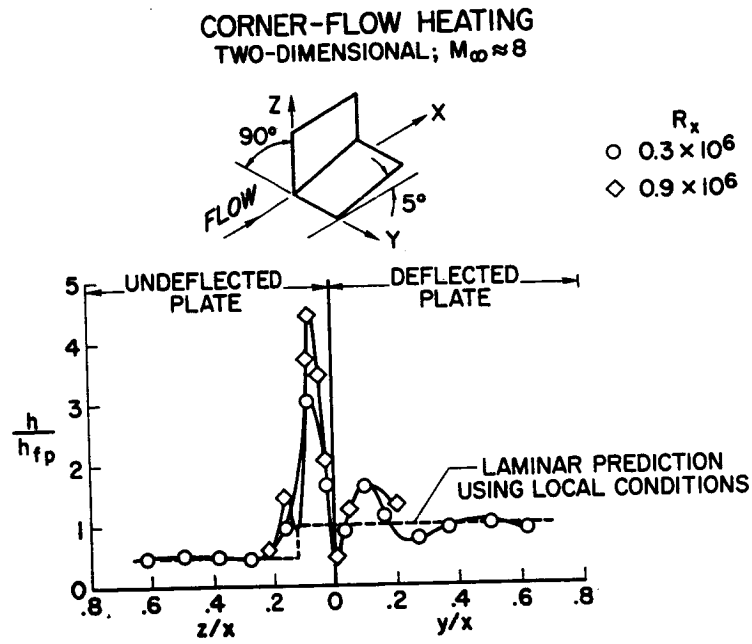
CORNER-FLOW HEATING
TWO-DIMENSIONAL; $M_\infty \approx 8$
Z
X
90°
FLOW
5°
Y
R_x
○ 0.3×10^6
◇ 0.9×10^6
UNDEFLECTED PLATE
DEFLECTED PLATE
$\frac{h}{h_{fp}}$
LAMINAR PREDICTION USING LOCAL CONDITIONS
z/x
y/x
(a)

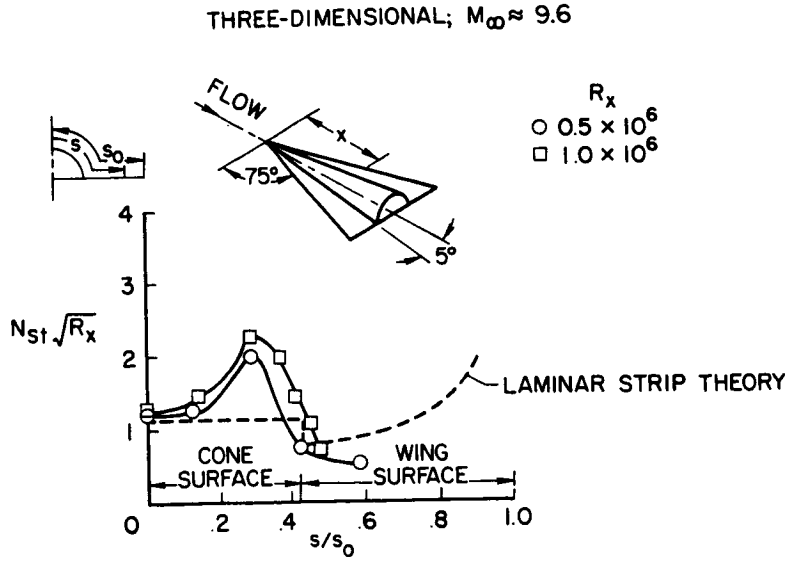
THREE-DIMENSIONAL; $M_\infty \approx 9.6$
FLOW
s
s_0
x
75°
5°
R_x
○ 0.5×10^6
□ 1.0×10^6
$N_{St}\sqrt{R_x}$
LAMINAR STRIP THEORY
CONE SURFACE
WING SURFACE
s/s_0
(b)

Figure 26

HEAT-SENSITIVE-PAINT RESULTS AT $M_\infty \approx 6.8$

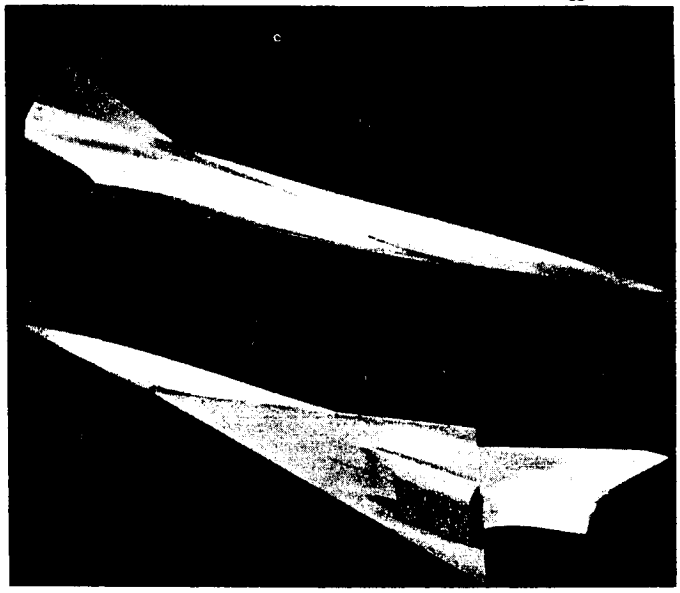

Figure 27 L-2697-22

POSSIBLE DESIGN CONCEPTS FOR HCV

VARIABLE GEOMETRY

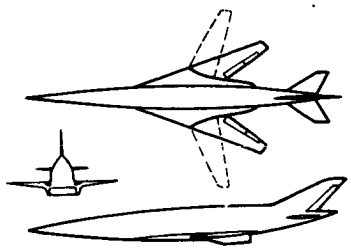

BLENDED WING-BODY

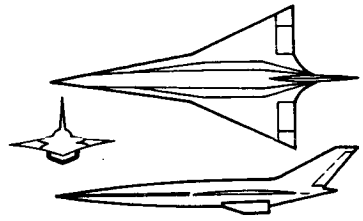

FIXED DELTA WING

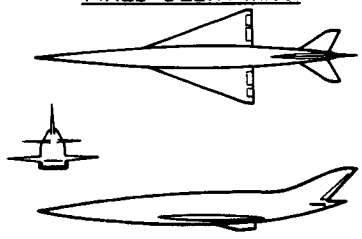

TWIST AND CAMBER

(a)

INTERFERENCE CONFIGURATION

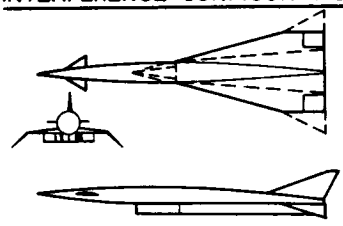

CARET WING

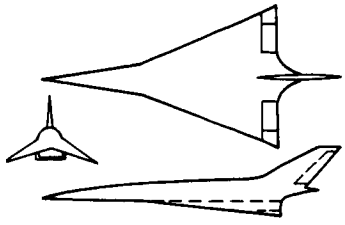

FLYING INLET ($M_\infty \approx 12$)

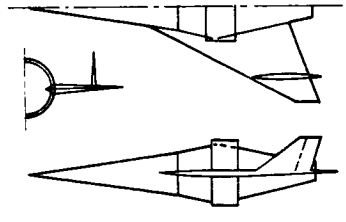

(b)

Figure 28

WIND-TUNNEL MODEL

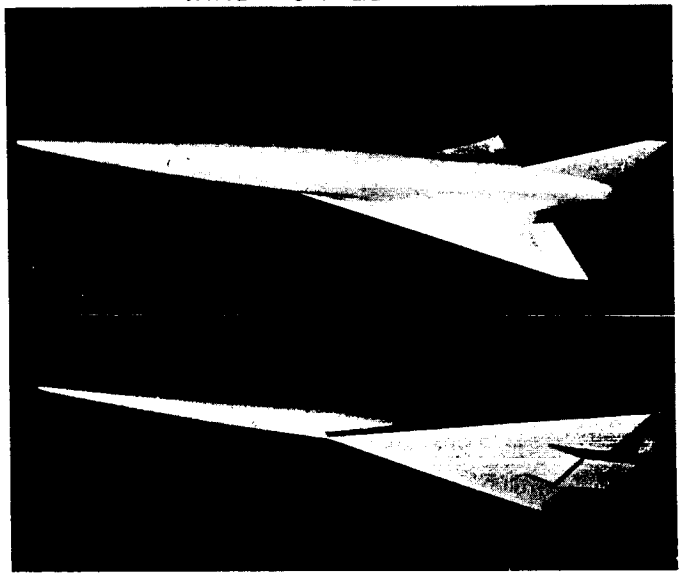

Figure 29 L-2697-21